Institut Pasteur
Microbes and Infection 16 (2014) 768–777
www.elsevier.com/locate/micinf

Original article

Role of dystrophin in acute *Trypanosoma cruzi* infection

Lygia M. Malvestio [a], Mara R.N. Celes [a,b,e], Cristiane Milanezi [c], João S. Silva [c], Linda A. Jelicks [d], Herbert B. Tanowitz [e], Marcos A. Rossi [a,1], Cibele M. Prado [a,e,*]

[a] *Department of Pathology, School of Medicine of Ribeirão Preto, University of São Paulo, SP, Brazil*
[b] *Institute of Tropical Pathology and Public Health, Federal University of Goiás, GO, Brazil*
[c] *Department of Biochemistry and Immunology, School of Medicine of Ribeirão Preto, University of São Paulo, SP, Brazil*
[d] *Department of Physiology and Biophysics, Albert Einstein College of Medicine, Bronx, NY, USA*
[e] *Department of Pathology, Albert Einstein College of Medicine, Bronx, NY, USA*

Received 26 March 2014; accepted 25 July 2014
Available online 4 August 2014

Abstract

Previous studies have demonstrated loss/reduction of dystrophin in cardiomyocytes in both acute and chronic stages of experimental *Trypanosoma cruzi* (*T. cruzi*) infection in mice. The mechanisms responsible for dystrophin disruption in the hearts of mice acutely infected with *T. cruzi* are not completely understood. The present in vivo and in vitro studies were undertaken to evaluate the role of inflammation in dystrophin disruption and its correlation with the high mortality rate during acute infection. C57BL/6 mice were infected with *T. cruzi* and killed 14, 20 and 26 days post infection (dpi). The intensity of inflammation, cardiac expression of dystrophin, calpain-1, NF-κB, TNF-α, and sarcolemmal permeability were evaluated. Cultured neonatal murine cardiomyocytes were incubated with serum, collected at the peak of cytokine production and free of parasites, from *T. cruzi*-infected mice and dystrophin, calpain-1, and NF-κB expression analyzed. Dystrophin disruption occurs at the peak of mortality and inflammation and is associated with increased expression of calpain-1, TNF-α, NF-κB, and increased sarcolemmal permeability in the heart of *T. cruzi*-infected mice at 20 dpi confirmed by in vitro studies. The peak of mortality occurred only when significant loss of dystrophin in the hearts of infected animals occurred, highlighting the correlation between inflammation, dystrophin loss and mortality.
© 2014 Institut Pasteur. Published by Elsevier Masson SAS. All rights reserved.

Keywords: *Trypanosoma cruzi*; Chagas disease; Dystrophin; Inflammation; Cardiomyocytes; Calpain-1

1. Introduction

Chagas disease, caused by *Trypanosoma cruzi*, remains an important neglected tropical disease and a cause of significant morbidity and mortality. The heart is severely and frequently involved in both acute and chronic stages of the disease. The cardiac involvement during the acute phase varies from mild to severe. Acute myocarditis is characterized by diffuse foci of myocytolytic necrosis and lymphomononuclear inflammatory infiltrate that spontaneously subsides after 2–3 months in most of cases. Clinical signs and symptoms are absent from most patients suffering from acute disease. In the indeterminate phase infected individuals are clinically asymptomatic. Thirty percent of these individuals will have clinically relevant chronic Chagas disease associated with chronic cardiomyopathy. This stages is associated with congestive heart failure and arrhythmias [1–5].

One of the most intriguing aspects of chronic Chagasic cardiomyopathy is the long delay after the initial infection to the chronic cardiac manifestations. This has been explained, in part, by our previous study demonstrating loss/reduction of dystrophin in mice experimentally infected with *T. cruzi*. Dystrophin immunolabeling was focally reduced or completely lost in cardiomyocytes 30 days post infection (dpi) and this reduction was maintained at 100 dpi. At 30 dpi there was an

* Corresponding author. Laboratory of Cellular and Molecular Cardiology, Department of Pathology, Faculty of Medicine of Ribeirão Preto, University of São Paulo, 14049-900 Ribeirão Preto, SP, Brazil.
E-mail address: cibeleprado@usp.br (C.M. Prado).
[1] Prof. Rossi died in 2013.

http://dx.doi.org/10.1016/j.micinf.2014.07.010
1286-4579/© 2014 Institut Pasteur. Published by Elsevier Masson SAS. All rights reserved.

intense acute myocarditis and ruptured or intact intracellular parasite nests, whereas at 100 dpi a mild chronic fibrosing myocarditis was detected with no parasites in the myocardium. Ejection fraction was reduced, the right ventricle was dilated and cardiac metabolism was altered at both time-points. Importantly, there was no correlation between myocyte necrosis or myocytolysis and dystrophin loss. These findings supported the hypothesis that the initial parasitic infection-induced myocardial reduction/loss of dystrophin significantly contributes to the delayed development of a cardiomyopathy [6].

It has been demonstrated that dystrophin loss destabilizes a complex of proteins present at the sarcolemma causing alteration in calcium homeostasis and increased membrane permeability, which may be related to impairment of contractile force transmission [7]. In addition, dystrophin reduction has been linked to the etiology of end-stage cardiomyopathies and has been proposed as a common pathway for the development of cardiomyopathy and congestive heart failure [8,9]. However, the mechanisms responsible for loss/reduction of dystrophin in the hearts of mice acutely infected with *T. cruzi* are not completely understood.

Dystrophin and many of the cytoskeletal proteins linking the cytoskeleton to the plasma membrane are rapidly cleaved by calcium-activated proteases, such as calpains [10]. It has been suggested that inflammation plays a role in the activation of calpains [11–14]. Since proinflammatory cytokine response is associated with the acute phase of Chagas disease [15–17], the present studies were undertaken to evaluate the role of inflammation in the loss/reduction of dystrophin and its association with the high mortality rate during acute infection.

2. Material and methods

2.1. Mice

Male C57Bl/6 mice aged 8–10 weeks (23–25 g) were maintained at a constant temperature (22 ± 2 °C) and a 12:12 h light–dark cycle. They were housed at the Animal Facility of the Department of Pathology of School of Medicine of Ribeirão Preto, University of São Paulo, and given standard mouse chow and water offered *ad libitum*. Primary culture of neonatal mouse cardiomyocytes was performed with myocytes obtained from neonatal C57Bl/6 mice from the breeding colony of Ribeirão Preto Medical School. All experimental procedures were conducted in accordance with international guidelines for the use of animals and received prior approval by the Committee on Animal Research of School of Medicine of Ribeirão Preto, University of São Paulo (Processes 06.1.428.53.9 and 183/2010) and complied with the Guide for the Care and Use of Laboratory Animals published by the National Institute of Health (NIH Publication No 85-23, revised 1996). All efforts were made to minimize animals suffering.

2.2. Experimental infection and blood collection

Mice were infected intraperitoneally with 1×10^3 trypomastigotes of the Y strain of *T. cruzi*. The Y strain of *T. cruzi* was maintained by serial passage from mouse to mouse. Parasitemia was individually checked by counting the number of parasites/5 μl of blood obtained from the tail vein from day 5 up to 30 dpi. At 12 dpi, peak of cytokines production [18,19], tail vein blood samples from infected and control mice were collected, centrifuged at 3000 rpm at 4 °C for 5 min, and the serum (free of parasites) stored at −80 °C for in vitro studies. Mortality was assessed daily and the mortality rate calculated.

2.3. In vivo experiments

2.3.1. Histopathological analysis

Animals were sacrificed 14, 20 and 26 dpi. The hearts were rapidly removed, rinsed in ice-cold 0.9% NaCl solution and fixed in neutral 10% formalin for histological study or immediately frozen in liquid nitrogen-cooled isopentane for evaluation of the membrane permeability, immunofluorescence and immunoblotting studies. Both ventricles from each heart were isolated and cut into two fragments by a mid-ventricular coronal section.

For histopathological study, the samples were dehydrated, clarified, embedded in paraffin, stained with hematoxylin and eosin and examined by light microscopy (n = 6/day/group). The tissue sections were used to evaluate the intensity of inflammation, the presence of amastigote nests and tissue damage.

For morphometric analysis, the number of interstitial mononuclear cells was counted as previously demonstrated [6] using the Leica QWin software (Leica Imaging Systems Ltd., Cambridge, England) in conjunction with a Leica microscope, video-camera, and an on-line (n = 6/day/group). Measurements were made by a skilled observed blinded to the groups.

2.3.2. Immunofluorescence

By immunofluorescence (IF) we evaluated dystrophin, calpain-1, TNF-α, and NF-κB expression at 14, 20 and 26 dpi. For IF microscopy, 5 μm frozen section (n = 6/day/group) were transferred to silane-coated slides and fixed in cold acetone for 10 min. Immunolabeling was performed using primary antibody to dystrophin (rabbit polyclonal antibody, Santa Cruz Biotechnology Inc., Santa Cruz, CA, USA, dilution 1:200), anti-calpain-1 (goat polyclonal antibody, 1:100; Santa Cruz Biotechnology), anti-TNF-α (mouse monoclonal antibody, 1:100; Santa Cruz Biotechnology) and anti-NF-κB (mouse monoclonal antibody, 1:100; Santa Cruz Biotechnology) diluted in 1% BSA and incubated *overnight* at 4 °C. Secondary antibodies fluorescein-conjugated anti-rabbit IgG, anti-goat IgG, or anti-mouse IgG, diluted 1:400 (Vector Laboratories Inc., Burlingame, CA, USA), were used. Omission of the primary antibodies served as negative control. F-actin filaments were stained with Alexa Fluor 594 (Invitrogen-GIBCO) for 1 h at room temperature and DNA was stained with DAPI (Molecular Probes). The images were analyzed with Leica DM 6000M microscope equipped with Leica AF6000 Deconvolution System (Leica Microsystems).

2.3.3. Immunoblotting

To determine the amount of dystrophin, calpain-1, TNF-α, and NF-κB in control and infected mice ($n = 5$/day/group), homogenates of the left and right ventricles were analyzed by immunoblotting at 14, 20 and 26 dpi. Hearts frozen at −80 °C were homogenized in extraction buffer with phosphatase and protease inhibitors (Sigma–Aldrich). Protein extract (50 μg protein/well) was separated on a 5% (dystrophin) or 10% (calpain-1, TNF-α, and NF-κB) polyacrylamide gel, and transferred to PVDF membrane (Hybond-ECL, Amersham Pharmacia Biotech, Amersham, UK). After blocking with 5% BSA/TBS-T for 24 h, the blots were incubated overnight at 4 °C with the antibody anti-dystrophin (rabbit polyclonal, 1:500, Santa Cruz Biotechnology Inc.), anti-calpain-1 (goat polyclonal, 1:500; Santa Cruz Biotechnology), anti-TNF-α (mouse monoclonal, 1:500; Santa Cruz Biotechnology), or anti-NF-κB (mouse monoclonal, 1:500; Santa Cruz Biotechnology). The blots were then washed and incubated with HRP-conjugated secondary antibodies for 40 min. The membranes were washed, developed with the ECL (Amersham Pharmacia Biotech) and gel documentation was made by Molecular Imager ChemiDoc XRS System (Bio-Rad, Richmond, CA, USA). Images were analyzed using the Image J program (National Institutes of Health, available at http://rbs.info.nih.gov/nih-image/), using the "gel analysis" function. Analysis of the value for each band, which is proportional to the integrated density value (IDV) of the band, corresponds to arbitrary units (AU). To control for lane loading, the same membranes were probed with tubulin (1:1000; Santa Cruz Biotechnology) or GAPDH (1:10,000, Cell Signaling, Danvers, MA, USA) after being washed with stripping buffer.

2.3.4. Assessment of membrane permeability

To assess changes in sarcolemmal membrane permeability of *T. cruzi*-infected mice at 20 dpi, Evans blue dye distribution was assessed. Evans blue dye is a nontoxic dye that binds to serum albumin when infused intravenously and allowed to recirculate. Evans blue dye cannot cross the sarcolemma of intact cardiomyocytes, but if the membrane is ruptured, it is found in the intracellular space where it binds to intracellular proteins. Intracellular staining of Evans blue dye therefore identifies increased membrane permeability or sarcolemmal damage [20]. Evans blue dye (Sigma–Aldrich, Inc., Saint Louis, MO, USA) was dissolved in PBS (10 mg/ml), sterilized through a 0.2 μm pore size filter, injected into the tail vein and kept circulating for 6 h before killing the animals. Cryosections were fixed in cold acetone at −20 °C for 10 min, washed with PBS, coverslipped in Vectashield Mounting Medium (Vector Laboratories). A double staining with Evans blue dye and dystrophin was performed to check if the cells that present dystrophin loss or reduction were the same cells that present permeability alteration. All sections were analyzed with Leica DM 6000M microscope equipped with Leica AF6000 Deconvolution System (Leica Microsystems). By fluorescence microscopy analysis, Evans blue dye staining showed a bright red emission and dystrophin showed a bright green emission.

2.4. In vitro experiments

2.4.1. Primary culture of neonatal mouse cardiomyocytes and treatments

In order to confirm in vivo results, in vitro experiments were performed using cultured neonatal cardiomyocytes.

Cardiomyocytes were isolated from neonatal mice hearts as previously described [21]. Briefly, 20 neonatal mice were killed by decapitation, the hearts were isolated and minced in the dissociation solution containing 1.25% pancreatin (GIBCO, Grand Island, NY, USA) and 300 mg/L bovine serum albumin (BSA; Sigma–Aldrich, Inc., St. Louis, MO, USA) diluted in (in g/L) 8.0 NaCl, 0.2 KCl, 0.05 Na_2HPO_4, 1.0 $NaHCO_3$, and 2.0 dextrose. The homogenate was transferred to an Erlenmeyer flask with the dissociation solution and placed in a water bath while continuously stirring. The supernatant fraction from each digestion period was spun at 1200 rpm for 10 min, and the pellet re-suspended in Dulbecco's modified Eagle's medium (DMEM) containing 10% fetal bovine serum (FBS) (GIBCO) and 1% penicillin/streptomycin (GIBCO). This procedure was repeated 5–7 times and then the tube with dissociated cells was placed in the incubator (37 °C, 5% CO_2). The cells were pooled and plated in 100 mm culture dishes for 2 h. Unattached 5×10^5 cells/cm^3 or 5×10^4 cells/cm^3 highly rich in myocytes were plated in 6-well cell culture plates (Corning, NY, USA) or in Permanox Lab-Teks chamber slides (Nalgene Nunc International, Rochester, NY, USA), respectively, and incubated for 24 h. After this period, the medium was replaced by DMEM supplemented with cytosine b-D-arabino-furanoside (Sigma–Aldrich) and the cultures incubated at 37 °C with 5% CO_2. After 5 days of incubation, the culture medium was removed and new medium supplemented with serum from either *T. cruzi*-infected or control mice and 10% FBS (v/v) was immediately added and left in the incubator for additional 24 h. Following the experimental periods, the cardiac cells were washed and processed for immunoblotting and IF labeling.

2.4.2. Immunofluorescence

Neonatal cardiomyocytes seeded in Lab-Teks chamber slides were incubated for 24 h with serum obtained from experimentally *T. cruzi*-infected and control mice at 12 dpi, as previously described. After incubation with filtered sera obtained from infected mice or control sera, cells were fixed with 4% paraformaldehyde for 20 min, and then washed three times with 4 °C cold PBS. Cells were permeabilized with 0.5% Triton X-100 (Sigma–Aldrich) and non-specific staining was blocked with 4% BSA. Primary antibodies to dystrophin (rabbit polyclonal antibody, 1:200; Santa Cruz Biotechnology), calpain-1 (goat polyclonal antibody, 1:100; Santa Cruz Biotechnology), NF-κB (mouse monoclonal antibody, 1:500; Santa Cruz Biotechnology) were incubated with the cells overnight at 4 °C. The cells were then washed and incubated with fluorescein-conjugated secondary antibodies. F-actin filaments and DAPI were stained as described previously. Images were analyzed as described above.

2.4.3. Immunoblotting

For measuring amounts of dystrophin and calpain-1 in cultured cardiomyocytes 24 h after incubation with filtered sera obtained from infected or control mice, the cells ($n = 3$ distinct cardiomyocytes cultures/group) were removed from plates and lysed with protease and phosphatase inhibitor cocktail (Sigma–Aldrich) using cell lifter. Total cell protein (20 μg of protein/well) was resolved on a 5% (dystrophin) or 10% (calpain-1) SDS-Page gel and transferred to PVDF membrane (Amersham Pharmacia Biotech, Amersham, UK). The membranes were blocked with 5% BSA/TBS-T for 2 h and incubated overnight at 4 °C with the primary antibodies anti-dystrophin (rabbit polyclonal antibody, 1:250; Santa Cruz Biotechnology) or anti-calpain-1 (goat polyclonal antibody, 1:250; Santa Cruz Biotechnology) followed by incubation with HRP-conjugated secondary antibodies for 40 min at room temperature. The loading control, documentation, and quantification of membranes were performed as previously described for in vivo studies.

2.5. Statistical analysis

In vivo and in vitro data were analyzed using a GraphPad Prism 5 statistics program (GraphPad Software Inc., San Diego, CA, USA). All data are presented as mean ± SD. Multiple comparisons were made using a one-way analysis of variance (ANOVA) followed by Bonferroni (parametric data) or Dunn's (nonparametric data) post hoc multiple-comparisons tests. For comparison of two groups Student's *t*-test was used. The survival rates were constructed using the Kaplan–Meier curve, and differences in mortality were compared using the log-rank (Mantel–Cox) test. A $p < 0.05$ was considered statistically significant.

3. Results

3.1. In vivo experiments

3.1.1. Parasitemia and mortality

Parasitemia was followed from 5 to 30 dpi. Mice exhibited progressively elevated parasitemia levels after 5 dpi, reaching the peak of 1.4×10^6 trypomastigotes/ml of plasma at 9 dpi. Twenty-six days after infection parasitemia waned. Mortality occurred between days 18 and 22 post infection, reaching the mortality peak of 50% at 20 dpi.

3.1.2. Histopathological analysis

Histological sections from hearts of *T. cruzi*-infected mice at 14 dpi displayed inflammatory infiltrate and rare amastigotes nests were observed. Isolated foci of fibrosis were observed. At 20 dpi, inflammatory infiltrates were more pronounced and rare amastigote nests were seen. Interstitial fibrosis was more evident. At 26 dpi, inflammation became significantly less intense and only sparse groups of infiltrating cells could still be observed; fibrosis was present. The quantification of the number of interstitial mononuclear cells demonstrated 41.4 ± 12 cells/field at 14 dpi, 53.4 ± 12 cells/field at 20 dpi and 36.42 ± 4 cells/field at 26 dpi in comparison with the number of interstitial mononuclear cells in control mice 22.3 ± 1.9 cells/field (Fig. 1).

3.1.3. Immunofluorescence and immunoblotting

The amount of dystrophin in the hearts of infected mice was markedly reduced at 20 dpi (0.18 ± 0.05 AU), representing a reduction of 65% ($p < 0.01$) compared to the amount of dystrophin in control mice (0.52 ± 0.03 AU). There were no differences in the amount of dystrophin 14 (0.45 ± 0.03 AU)

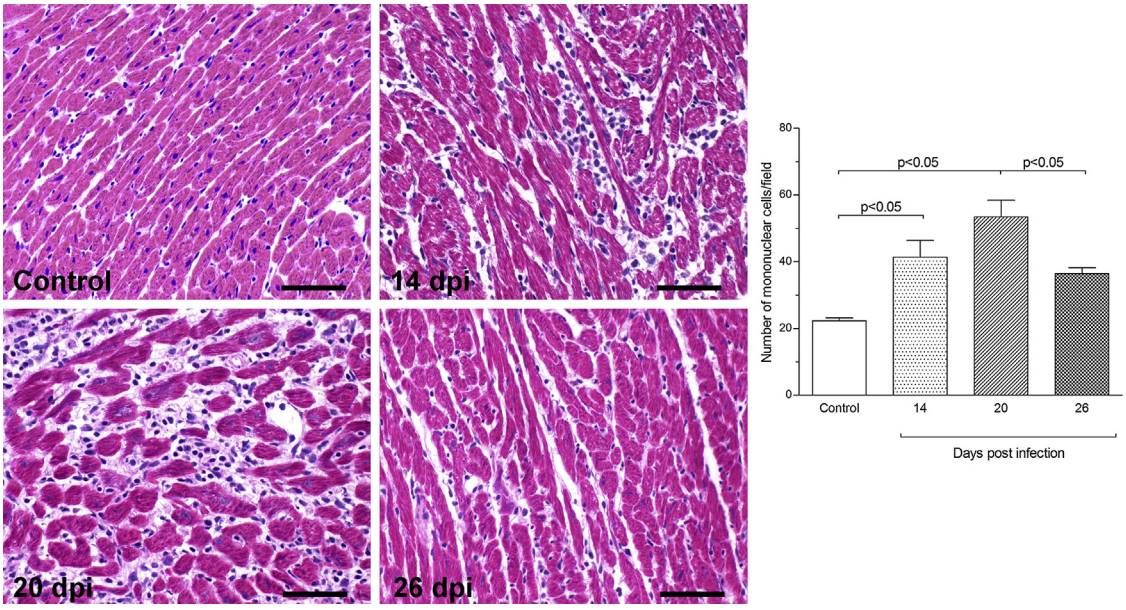

Fig. 1. Histological analysis of left ventricle. Control mice displayed normal cardiac fibers with regular interstitial space. At 14 dpi there was a diffuse myocarditis characterized by lymphomononuclear interstitial infiltrate and enlargement of the interstitial space. At 20 dpi inflammation was even more intense. After 26 dpi, the number of lymphomononuclear inflammatory cells decreased and no parasites were observed. Bars = 60 microns.

and 26 dpi (0.29 ± 0.05 AU) compared to control mice. The IF revealed that dystrophin immunolabeling occurred in a uniform pattern as a continuous rim at the periphery of most cardiomyocytes (Fig. 2, green fluorescence). However, dystrophin expression was focally lost in some foci of cardiomyocytes mainly at 20 dpi (Fig. 2, head arrows). In order to determine whether dystrophin loss was a consequence of cardiomyocyte death, the sections were double-stained against F-actin to detect cardiomyocyte cytoskeletal F-actin (Fig. 2, red fluorescence). Spread blocks of cardiomyocytes lacking dystrophin distinctly showed the red fluorescent signal for F-actin, indicating an absence of correlation between myocyte necrosis or myocytolysis and dystrophin loss. Moreover, some amastigote nests were seen at 14 and 20 dpi (Fig. 2, arrows).

The amount of calpain-1 was significantly increased at 14 (0.38 ± 0.03 AU) and 20 (0.34 ± 0.07 AU) dpi, representing an increase of approx. 90% and 70% ($p < 0.05$), respectively, compared to the amount of calpain-1 in control mice (0.20 ± 0.01 AU). There was no difference of calpain-1 at 26 dpi (0.24 ± 0.01 AU) as compared to control animals (Fig. 3C). The IF signal for calpain-1 progressively increased at 14 and 20 dpi (Fig. 3B, green fluorescence), and was associated with an increased number of inflammatory cells as revealed by blue fluorescence of DAPI when compared with control mice (Fig. 3A).

The NF-κB amounts were increased at 14 (0.77 ± 0.13 AU) and 20 dpi (0.76 ± 0.15), representing an increase of approx. 133% and 130% ($p < 0.05$), respectively, when compared with mean amounts of NF-κB in control animals (0.33 ± 0.02 AU). There was no difference of NF-κB at 26 dpi (0.58 ± 0.17 AU) as compared to control animals (Fig. 3F). The IF revealed that NF-κB peaked at 14 and 20 dpi (Fig. 3E, green fluorescence) and was associated with increased number of inflammatory cells as revealed by blue fluorescence of DAPI in comparison with control mice (Fig. 3D). Similarly, the amount of TNF-α was significantly increased at 14 (0.38 ± 0.04 AU) and 20 dpi (0.44 ± 0.08 AU), representing an increase of approximately 80% and 109%, respectively, in comparison with the amount of TNF-α in control mice (0.21 ± 0.04 AU). There was no difference of TNF-α at 26 dpi (0.25 ± 0.05 AU) as compared to control mice (Fig. 3I). The TNF-α fluorescence peak was at 14 and 20 dpi (Fig. 3H, green fluorescence) and was almost absent in control mice (Fig. 3G, green fluorescence). Cardiomyocytes were stained for F-actin (red fluorescence).

3.1.4. Sarcolemmal permeability evaluated by Evans blue dye

The assessment of sarcolemmal permeability with Evans blue dye showed that *T. cruzi*-infected mice presented with more permeable sarcolemma. In control animals, there was no intracellular staining with Evans blue dye. However, cardiomyocytes from infected mice at 20 dpi presented a bright red fluorescence in the cytoplasm of spread blocks cells, indicating that structural perturbation of the plasma membrane integrity was seen (Fig. 4, red fluorescence). The merge of dystrophin and Evans blue images shows that cardiomyocytes presenting Evans blue staining were the same as those with dystrophin loss (Fig. 4, head arrow).

3.2. In vitro results

3.2.1. Immunofluorescence and immunoblotting

Neonatal cardiomyocytes were evaluated following a period of 24 h after incubation with filtered sera obtained from infected or control mice [(10% (v/v)]. The IF analysis clearly showed decreased expression of dystrophin associated with

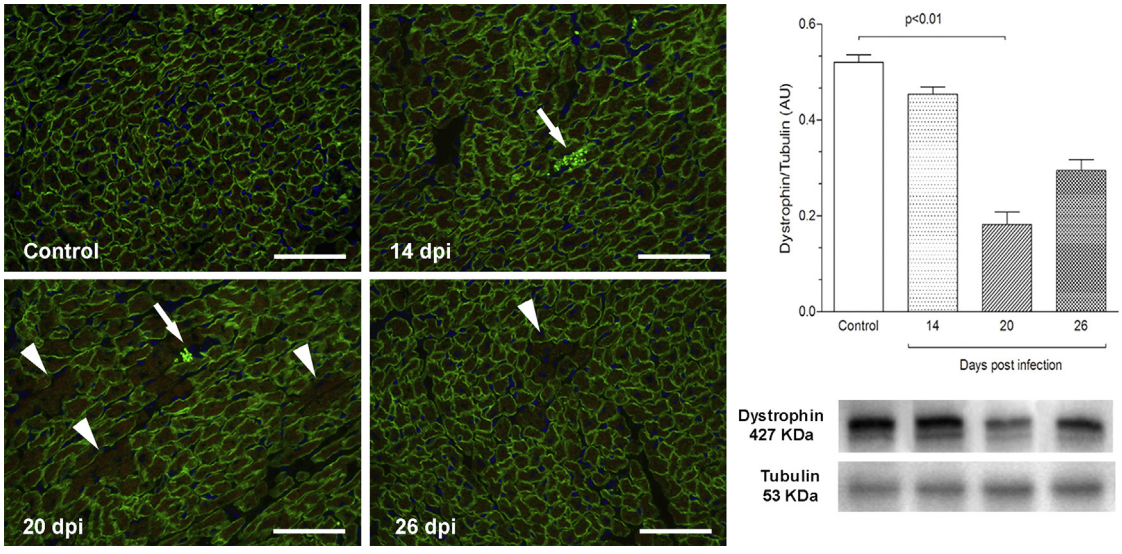

Fig. 2. Representative images of IF for dystrophin in control and *T. cruzi*-infected mice and immunoblotting quantification. The IF study showed that dystrophin labeling occurred in a uniform pattern as a continuous rim at the periphery of most cardiomyocytes (green fluorescence). Dystrophin expression was focally lost in some foci of cardiomyocytes mainly at 20 dpi (head arrows). The red fluorescence signal shows staining for F-actin. Some amastigote nests are seen at 14 and 20 dpi (arrows). Densitometric analysis of immunoblotting showed a significant reduction of dystrophin at 20 dpi. Tubulin signal was used to normalize loading differences between lanes. Bars = 60 microns.

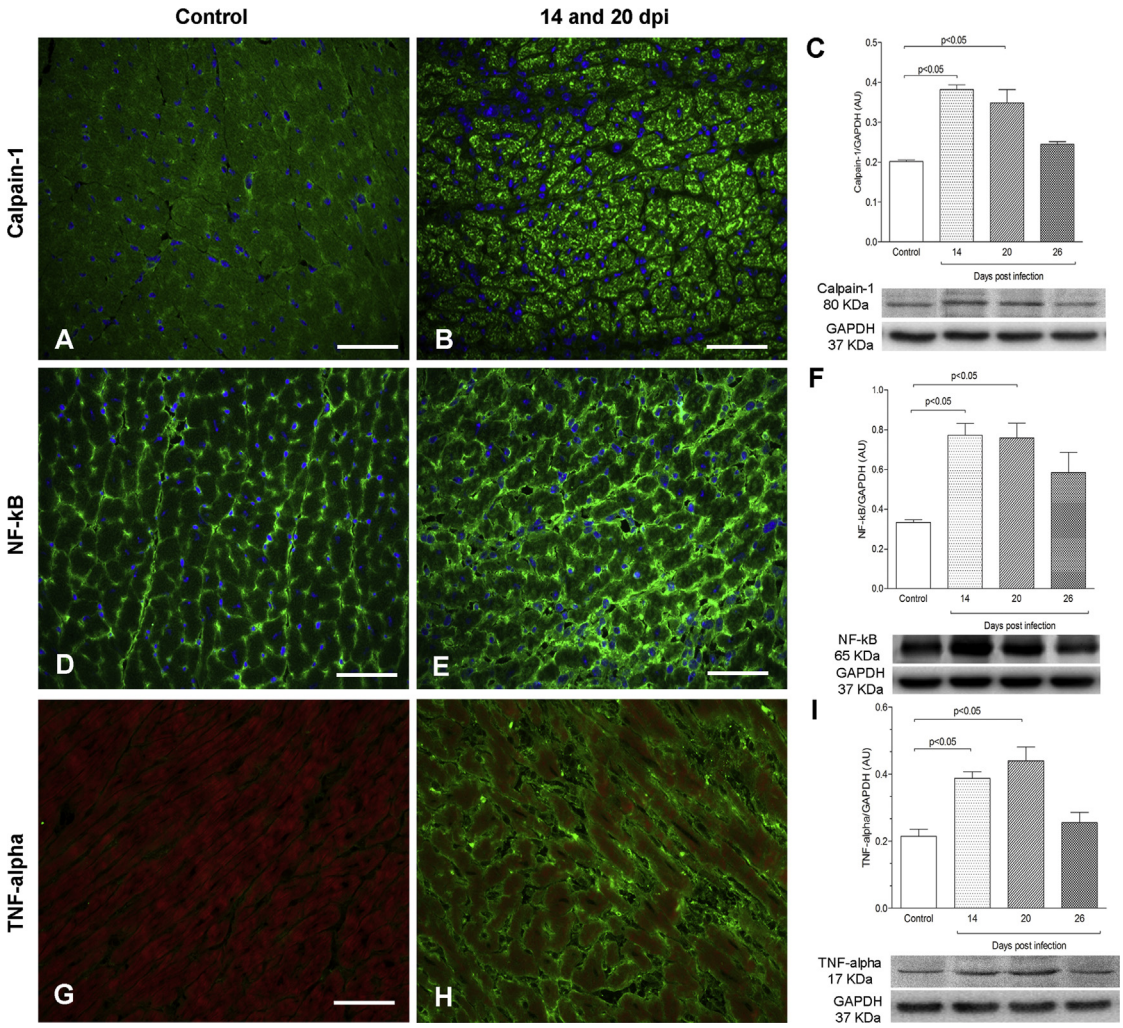

Fig. 3. Representative images of IF for calpain-1, NF-kB and TNF-alpha in control and *T. cruzi*-infected mice and immunoblotting quantification. The IF signal for calpain-1 was increased peaking at 14 and 20 dpi (green fluorescence), associated with increased number of inflammatory cells revealed by blue fluorescence of DAPI when compared with control mice. The immunoblotting quantification corroborates the IF findings. The same phenomenon was observed in the IF signal for NF-kB (green fluorescence). The TNF-alpha IF signal (green fluorescence) was quite weak in control mice as compared to infected mice. F-actin is showed in red. GAPDH signal was used to normalize loading differences between lanes in the WB quantification. Bars = 60 microns.

cytoplasmic vacuolization and formation of multiple blebs dispersed in the cytoplasm of cardiomyocytes incubated with filtered sera obtained from infected mice (Fig. 5D, green fluorescence) as compared to that observed in cardiomyocytes incubated with control sera (Fig. 5A). F-actin fluorescence staining revealed disruption and rearrangement of filaments (Fig. 5E, red fluorescence), as compared to control (Fig. 5B). The quantification of dystrophin by immunoblotting showed a reduction of 50% (1.6 ± 0.32 AU) in cultured cardiomyocytes incubated with filtered sera obtained from infected mice in comparison to those incubated with control sera (0.8 ± 0.21 AU), corroborating the IF findings (Fig. 5).

Cultured neonatal mouse cardiomyocytes incubated with filtered sera obtained from infected mice presented increased fluorescence expression of calpain-1 (Fig. 6D, green fluorescence) in comparison with cardiomyocytes incubated with control sera (Fig. 6A). Immunoblotting results demonstrated that the amount of calpain-1 was increased by approx. 33% (1.6 ± 0.04 AU) in cardiomyocytes incubated with filtered sera obtained from infected mice in comparison with values in control cardiomyocytes (1.2 ± 0.06 AU) (Fig. 6).

Cultured cardiomyocytes incubated with filtered sera obtained from infected mice displayed a marked increased fluorescence of NF-κB (Fig. 6J) in comparison with cardiomyocytes incubated with control sera (Fig. 6G). In addition, disruption and rearrangement of F-actin associated with reduced size of cardiomyocytes were observed after the addition of filtered sera obtained from infected mice (Fig. 6L) as compared to control sera (Fig. 6H).

4. Discussion

The present study demonstrates that loss/reduction of cardiac dystrophin occurs at the peak of mortality and inflammation, increased expression of calpain-1, TNF-α, NF-κB, and increased sarcolemmal permeability in the heart of *T. cruzi*-infected. These data were confirmed by in vitro studies where serum of *T. cruzi*-infected mice, collected at the peak of

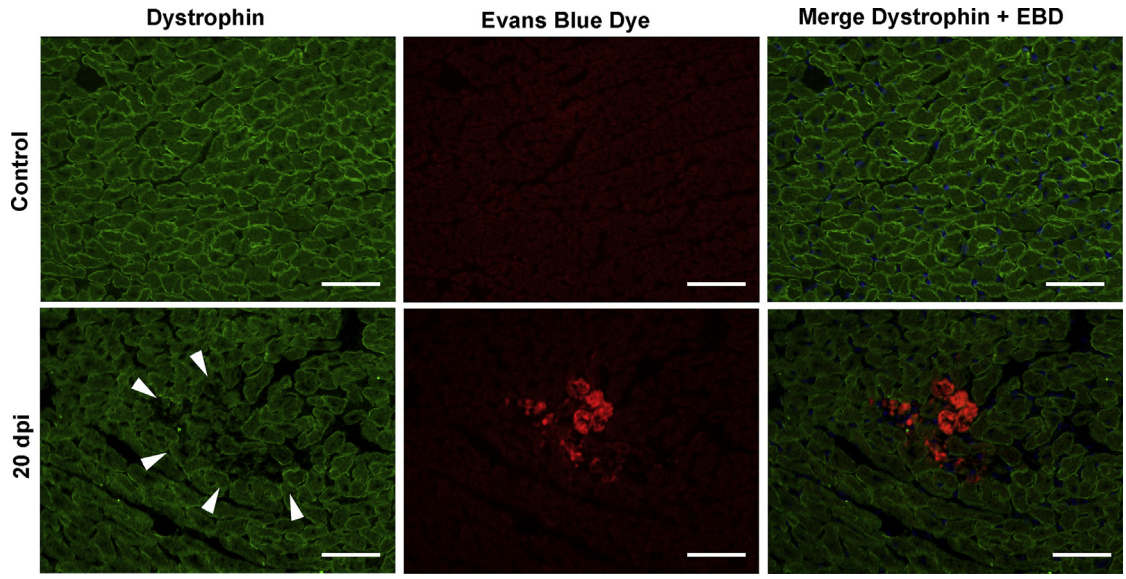

Fig. 4. Representative images of IF for dystrophin (green fluorescence) and Evans blue dye uptake (red fluorescence). The assessment of sarcolemmal permeability with Evans blue dye showed that *T. cruzi*-infected mice present more permeable sarcolemma. In control animals, there was no intracellular staining with Evans blue dye. At 20 dpi a bright red fluorescence in the cytoplasm of spread blocks of cardiomyocytes was seen. The merge of dystrophin and Evans blue images shows that cardiomyocytes presenting Evans blue staining were the same of those with dystrophin loss (head arrow). Bars = 60 microns.

cytokine production and free of parasites, was incubated with cultured neonatal cardiomyocytes. It is noteworthy that although there is no difference among the expression of calpain-1, TNF-α and NF-κB between 14 and 20 dpi, the peak of mortality occurred only when significant loss of dystrophin in the hearts of infected animals occurred, highlighting the correlation between inflammation, dystrophin loss and mortality.

Our results demonstrated a marked inflammatory infiltrate associated with interstitial fibrosis and rare amastigote nests in the hearts of mice infected with Y strain of *T. cruzi* at 14 and mainly at 20 dpi. During acute infection there is an intense inflammatory response associated with an upregulation of pro-inflammatory mediators [17,22]. As a result of this focal mononuclear cell inflammation, a 2-fold increase of TNF-α was detected by immunoblotting and IF in the hearts of mice infected with *T. cruzi* at 20 dpi. It has been proposed that inflammatory cytokines stimulate endoplasmic reticulum release of Ca^{+2}, resulting in activation of calcium-activated proteases, that produces further intracellular changes, including

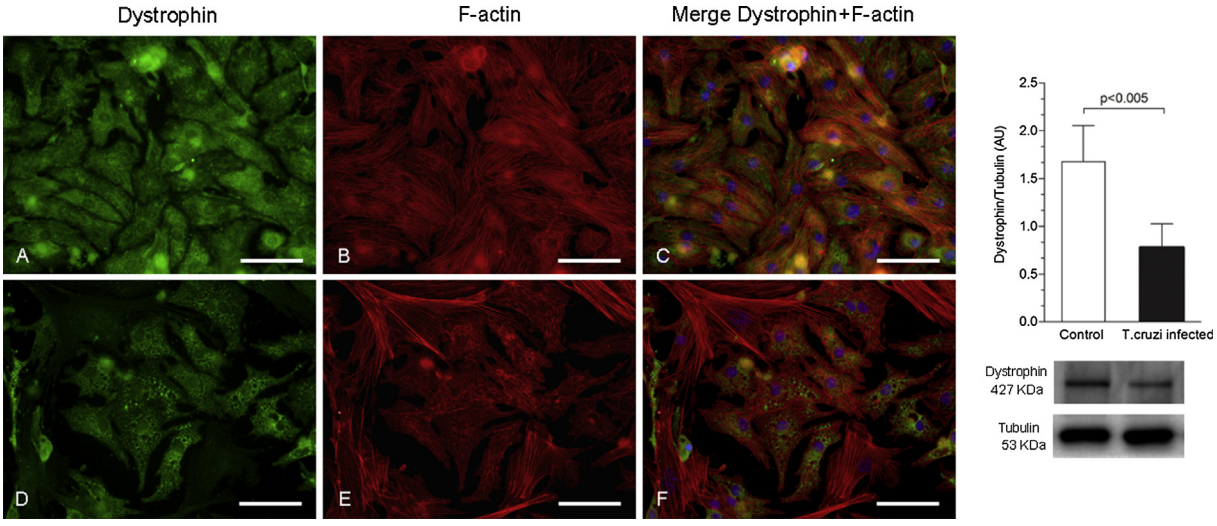

Fig. 5. Representative images of IF for dystrophin (green fluorescence) and immunoblotting quantification in cultured newborn cardiomyocytes incubated with control sera (A,B,C) or incubated with filtered sera obtained from infected mice (D,E,F). F-actin was stained with Alexa fluor 594 (red fluorescence) and nuclei with DAPI (blue fluorescence). Cardiomyocytes incubated with filtered sera obtained from infected mice presented bleb formation and decreased expression of dystrophin (D) and disruption and rearrangement of filaments (E and F) as compared to dystrophin expression in control cardiomyocytes (A). Immunoblotting quantification demonstrated that the amount of dystrophin was markedly decreased, by ~50%, in cardiomyocytes incubated with filtered sera obtained from infected mice compared to amounts observed in control cardiomyocytes. Tubulin was used as a protein loading control. Bars = 50 microns.

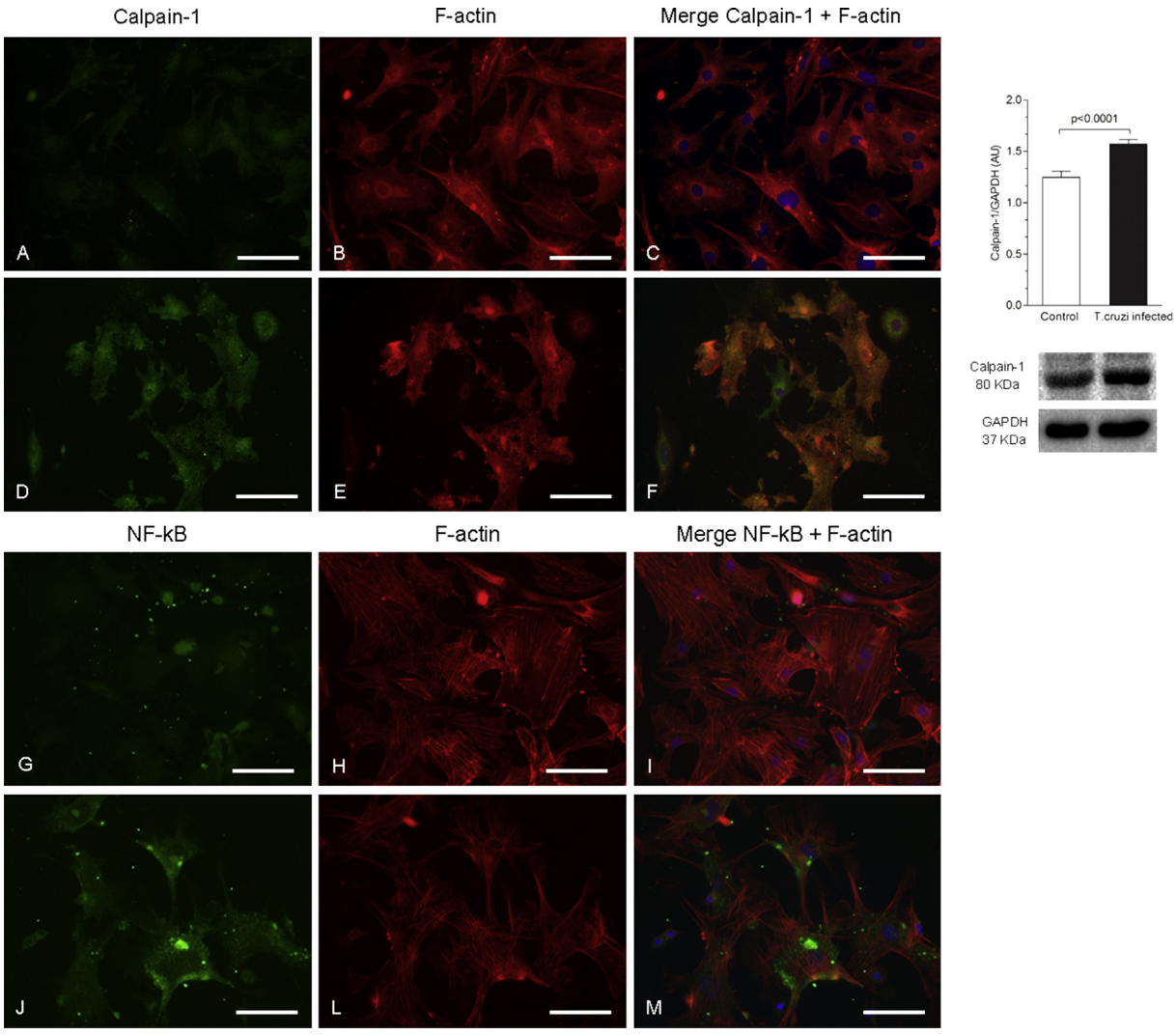

Fig. 6. Representative IF images for calpain-1 and NF-kB (green fluorescence) and immunoblotting quantification in cultured newborn cardiomyocytes incubated with control sera (A,B,C,G,H,I) or with filtered sera obtained from infected mice (D,E,F,J,L,M). F-actin was stained with Alexa fluor 594 (red fluorescence) and nuclei with DAPI (blue fluorescence). Cardiomyocytes incubated with filtered sera obtained from infected mice presented increased expression of calpain-1 as compared to expression levels in control cardiomyocytes (A). In merged images, cardiomyocytes incubated with filtered sera obtained from infected mice are orange (F, green and red mixed) while control cardiomyocytes remain red (C). Immunoblotting quantification demonstrated that calpain-1 amount was markedly increased, by ~33%, in cardiomyocytes incubated with filtered sera obtained from infected mice compared to amounts observed in control cardiomyocytes. GAPDH was used as a protein loading control. The IF signal for NF-κB is strikingly increased (J) in cardiomyocytes incubated with filtered sera obtained from infected mice in comparison with the IF signal in control cardiomyocytes (G). A disarrangement of filaments associated with reduced size of cardiomyocytes was evidenced by F-actin fluorescence staining (L). Bars = 50 microns.

secondary inflammation [11,12]. In addition to increased TNF-α level, increased levels of NF-κB were observed both in vivo and in vitro studies. NF-κB is a transcription factor that regulates expression of genes mainly involved in the inflammatory response and the immune system [23]. Its activation occurs through degradation of its inhibitory protein IκB-α and NF-κB translocation to the nucleus [23–25]. Once activated, NF-κB triggers an enhanced expression of cytokines, thereby initiating a vicious cycle in a positive feedback loop [26–29].

The IF findings demonstrate an increased expression of the calcium-activated protease calpain-1 in the hearts of mice infected with the parasite *T. cruzi* as compared to control mice. This data was confirmed in cardiomyocytes incubated with filtered sera obtained from infected mice as compared to cardiomyocytes incubated with control sera. Calpains require micromolar or millimolar Ca^{+2} concentrations for activity. Many of the proteins linking the cytoskeleton to the plasma membrane are cleaved rapidly by the calpains, including dystrophin [10]. In addition, increased calpain activity has often been reported as an aggravating factor in cardiovascular diseases and other pathophysiological conditions [30].

In the present study, the amount of dystrophin was markedly reduced at 20 dpi in the hearts of *T. cruzi*-infected mice as compared to control mice. The same phenomenon was observed in cardiomyocytes incubated with filtered sera obtained from infected mice as compared to cardiomyocytes incubated with control sera. These alterations were corroborated by immunoblotting results showing a marked decreased in dystrophin level

in both situations. This decrease could be a direct consequence of calcium-dependent calpain activity that cleaves dystrophin very rapidly when calcium concentration is compatible with this activation [10,31]. This assertion is reinforced by observation of coincidental findings between peaks of dystrophin disruption and calpain-1 expression in both in vivo and in vitro studies. Absence of dystrophin results in the rupture of the physical linkage of the subsarcolemmal cytoskeleton to the sarcolemma, thus impairing contractile transmission and resulting in contractile dysfunction. Concomitantly, this breakdown of the link with the cytoskeleton may impair the sarcolemmal integrity and increase fragility and permeability [17,32]. The alteration in membrane permeability was confirmed with double staining of dystrophin and Evans blue dye in the cardiomyocytes of infected mice at 20 dpi. The cells that have Evans blue dye red fluorescence in the cytoplasm were the same cells that have lost dystrophin expression.

Another important finding is the cell shape change with cytoplasmic vacuolization and bleb formation in the cardiomyocytes incubated with filtered sera obtained from infected mice. Studies using renal tubule cells of rabbit and hepatocytes of rats exposed to highly toxic agents that act by increasing cytosolic calcium levels have shown that intracellular concentrations of calcium precede bleb formation. Pretreatment of these cells with protease inhibitor prevented bleb formation but also decreased proteolysis rate [33–35]. The activation of calcium-dependent proteases could be responsible for the rearrangement of F-actin filaments inducing the formation of bubbles [36]. These findings emphasize the role of proinflammatory cytokines present in the serum of animals experimentally infected with *T. cruzi*, in the activation of calcium-dependent proteases.

In summary, although the levels of calpain-1, TNF-α, NF-κB were increased in the mice infected with *T. cruzi* as compared to control mice at 14 and 20 dpi, only when cardiac dystrophin expression was significantly decreased was the peak of mortality observed. This underscores the relationship between inflammation, dystrophin loss and mortality. In another study, the disruption of dystrophin has been suggested to contribute to sudden death of patients who suffered myocardial infarction [37]. Our in vitro studies employing cultured neonatal cardiomyocytes incubated with filtered sera obtained from infected mice, confirmed the in vivo findings that calpain-1 could be responsible for the dystrophin reduced expression. Further studies are needed to shed light on this mechanism such as the use of specific calpain inhibitors. These studies could provide novel therapeutic targets to prevent death during acute Chagas disease.

Acknowledgments

The authors thank Lígia B. Santoro, Maria E. Riul, Mônica A. Abreu, Vicki L. Braunstein and Dazhi Zhao for excellent technical assistance. This study was supported by grants from the Fundação de Amparo à Pesquisa do Estado de São Paulo (FAPESP 09/17787-8; 10/19216-5; 10/18629-4; 06/52882-3; 06/59618-0), National Institutes of Health AI076248 and by Fogarty International Training grant D43-TW007129.

References

[1] Köberle F. Chagas' disease and Chagas' syndromes: the pathology of American trypanosomiasis. Adv Parasitol 1968;6:63–116.
[2] Rossi MA. Microvascular changes as a cause of chronic cardiomyopathy in Chagas' disease. Am Heart J 1990;120:233–6.
[3] Rossi MA, Bestetti RB. The challenge of chagasic cardiomyopathy. The pathologic roles of autonomic abnormalities, autoimmune mechanisms and microvascular changes, and therapeutic implications. Cardiology 1995;86:1–7.
[4] Tanowitz HB, Machado FS, Jelicks LA, Shirani J, de Carvalho AC, Spray DC, et al. Perspectives on *Trypanosoma cruzi*-induced heart disease (Chagas disease). Prog Cardiovasc Dis 2009;51:524–39.
[5] Rossi MA, Tanowitz HB, Malvestio LM, Celes MR, Campos EC, Blefari V, et al. Coronary microvascular disease in chronic Chagas cardiomyopathy including an overview on history, pathology, and other proposed pathogenic mechanisms. PLoS Negl Trop Dis 2010;4:e674.
[6] Prado CM, Celes MR, Malvestio LM, Campos EC, Silva JS, Jelicks LA, et al. Early dystrophin disruption in the pathogenesis of experimental chronic Chagas cardiomyopathy. Microbes Infect 2012;14:59–68.
[7] Danialou G, Comtois AS, Dudley R, Karpati G, Vincent G, Des Rosiers C, et al. Dystrophin-deficient cardiomyocytes are abnormally vulnerable to mechanical stress-induced contractile failure and injury. FASEB J 2001;15:1655–7.
[8] Kawada T, Masui F, Tezuka A, Ebisawa T, Kumagai H, Nakazawa M, et al. A novel scheme of dystrophin disruption for the progression of advanced heart failure. Biochim Biophys Acta 2005;1751:73–81.
[9] Toyo-Oka T, Kawada T, Nakata J, Xie H, Urabe M, Masui F, et al. Translocation and cleavage of myocardial dystrophin as a common pathway to advanced heat failure: a scheme for the progression of cardiac dysfunction. Proc Natl Acad Sci U S A 2004;101:7381–5.
[10] Goll DE, Thompson VF, Li H, Wei W, Cong J. The calpain system. Physiol Rev 2003;83:731–801.
[11] Nozaki K, Das A, Ray SK, Banik NL. Calpain inhibition attenuates intracellular changes in muscle cells in response to extracellular inflammatory stimulation. Exp Neurol 2010;225:430–5.
[12] Nozaki K, Das A, Ray SK, Banik NL. Calpeptin attenuated apoptosis and intracellular inflammatory changes in muscle cells. Neurosci Res 2011;89:536–43.
[13] Letavernier E, Perez J, Bellocq A, Mesnard L, Keller AC, Haymann JP, et al. Targeting the calpain/calpastatin system as a new strategy to prevent cardiovascular remodeling in angiotensin II induced hypertension. Circ Res 2008;102:720–8.
[14] Ruetten H, Thiemermann C. Effect of calpain inhibitor I, an inhibitor of the proteolysis of I kappa B, on the circulatory failure and multiple organ dysfunction caused by endotoxin in the rat. Br J Pharmacol 1997;121:695–704.
[15] Tarleton RL. Tumor necrosis factor (cachectin) production during experimental Chagas' disease. Clin Exp Immunol 1988;73:186–90.
[16] Zhang L, Tarleton RL. Persistent production of inflammatory and anti-inflammatory cytokines and associated MHC and adhesion molecule expression at the site of infection and disease in experimental *Trypanosoma cruzi* infections. Exp Parasitol 1996;84:203–13.
[17] Chandrasekar B, Melby PC, Troyer DA, Colston JT, Freeman GL. Temporal expression of pro-inflammatory cytokines and inducible nitric oxide synthase in experimental acute chagasic cardiomyopathy. Am J Pathol 1998;152:925–34.
[18] Starobinas N, Russo M, Minoprio P, Hontebeyrie-Joskowicz M. Is TNF alpha involved in early susceptibility of *Trypanosoma cruzi*-infected C3H/He mice? Res Immunol 1991;142:117–22.
[19] Panis C, Mazzuco TL, Costa CZF, Victorino VJ, Tatakihara VLH, Yamauchi LM, et al. *Trypanosoma cruzi*: effect of the absence of 5-lipoxygenase (5-LO)-derived leukotrienes on levels of cytokines, nitric

oxide and iNOS expression in cardiac tissue in the acute phase of infection in mice. Exp Parasitol 2011;127:58–65.
[20] Matsuda R, Nishikawa A, Tanaka H. Visualization of dystrophic muscle fibers in mdx mouse by vital staining with Evans blue: evidence of apoptosis in dystrophin-deficient muscle. J Biochem 1995;118:959–64.
[21] Celes MR, Malvestio LM, Suadicani SO, Prado CM, Figueiredo MJ, Campos EC, et al. Disruption of calcium homeostasis in cardiomyocytes underlie cardiac structural and functional changes in severe sepsis. PLoS One 2013;8:e68809.
[22] Andrade ZA. Pathogenesis of Chagas' disease. Res Immunol 1991;142:126–9.
[23] Kumar A, Takada Y, Boriek AM, Aggarwal BB. Nuclear factor-kappaB: its role in health and disease. J Mol Med (Berl) 2004;82:434–48.
[24] Kumar A, Boriek AM. Mechanical stress activates the nuclear factor-kappaB pathway in skeletal muscle fibers: a possible role in duchenne muscular dystrophy. FASEB J 2003;17:386–96.
[25] Messina S, Bitto A, Aguennouz M, Minutoli L, Monici MC, Altavilla D, et al. Nuclear factor kappa-B blockade reduces skeletal muscle degeneration and enhances muscle function in mdx mice. Exp Neurol 2006;198:234–41.
[26] Valen G, Yan ZQ, Hansson GK. Nuclear factor kappa-B and the heart. J Am Coll Cardiol 2001;38:307–14.
[27] Huang H, Calderon TM, Berman JW, Braunstein VL, Weiss LM, Wittner M, et al. Infection of endothelial cells with *Trypanosoma cruzi* activates NF-kappaB and induces vascular adhesion molecule expression. Infect Immun 1999;67:5434–40.
[28] Huang H, Chan J, Wittner M, Jelicks LA, Morris SA, Factor SM, et al. Expression of cardiac cytokines and inducible form of nitric oxide synthase (NOS2) in *Trypanosoma cruzi*-infected mice. J Mol Cell Cardiol 1999;31:75–88.
[29] Huang H, Petkova SB, Cohen AW, Bouzahzah B, Chan J, Zhou JN, et al. Activation of transcription factors AP-1 and NF-kappa B in murine Chagasic myocarditis. Infect Immun 2003;71:2859–67.
[30] Sorimachi H, Ono Y. Regulation and physiological roles of the calpain system in muscular disorders. Cardiovasc Res 2012;96:11–22.
[31] Cottin P, Poussard S, Mornet D, Brustis JJ, Mohammadpour M, Leger J, et al. In vitro digestion of dystrophin by calcium-dependent proteases, calpains I and II. Biochimie 1992;74:565–70.
[32] Rodríguez M, Cai WJ, Kostin S, Lucchesi BR, Schaper J. Ischemia depletes dystrophin and inhibits protein synthesis in the canine heart: mechanisms of myocardial ischemic injury. J Mol Cell Cardiol 2005;38:723–33.
[33] Armstrong SC, Shivell LC, Ganote CE. Sarcolemmal blebs and osmotic fragility as correlates of irreversible ischemic injury in preconditioned isolated rabbit cardiomyocytes. J Mol Cell Cardiol 2001;33:149–60.
[34] Smith MW, Phelps PC, Trump BF. Cytosolic Ca2+ deregulation and blebbing after HgCl2 injury to cultured rabbit proximal tubule cells as determined by digital imaging microscopy. Proc Natl Acad Sci U S A 1991;88:4926–30.
[35] Nicotera P, Hartzell P, Davis G, Orrenius S. The formation of plasma membrane blebs in hepatocytes exposed to agents that increase cytosolic Ca2+ is mediated by the activation of a non-lysosomal proteolytic system. FEBS Lett 1986;209:139–44.
[36] Elliget KA, Phelps PC, Trump BF. HgCl2-induced alteration of actin filaments in cultured primary rat proximal tubule epithelial cells labelled with fluorescein phalloidin. Cell Biol Toxicol 1991;7:263–80.
[37] Andréoletti L, Ventéo L, Douche-Aourik F, Canas F, Lorin de la Grandmaison G, Jacques J, et al. Active coxsackieviral B infection is associated with disruption of dystrophin in endomyocardial tissue of patients who died suddenly of acute myocardial infarction. J Am Coll Cardiol 2007;50:2207–14.